

Species occurrence as a function of both emergent biological traits
and environmental context

Peter D. Smits^{1,*}

1. University of Chicago, Chicago, Illinois 60637.

* Corresponding author; e-mail: psmits@uchicago.edu.

Manuscript elements:

Keywords:

Manuscript type: Article

Prepared using the suggested L^AT_EX template for *Am. Nat.*

Introduction

- 2 How do species pools change over time as species are recruited or go extinct? When are ecotypes enriched or depleted? How does global and regional environmental context affect the distribution of
- 4 species ecotypes (e.g. guilds) in a regional species pool?

A regional species pool is the set of species which form communities in a specific region; local communities are subsets of the regional pool. The composition of a regional species pool changes over time due to speciation, migration, extinction. Local scale processes like resource competition

6
8 only affect the regional species pool if all communities are affected.

Valentine and Bambach how they presented guilds in paleobiology which is taxa united by similarity of their macroecology (Bambach, 1977; Valentine, 1969). Bush and Bambach presented an ecocube to describe what how marine invertebrates partition space and resources (Bambach et al., 2007; Bush and Bambach, 2011; Bush et al., 2007). Unique combinations represent what possible ecotypes are observable. The distribution of ecocube occupancy is then normally analyzed as raw counts of unique combinations or using ordination methods and the change in disparity over time is estimated (Bambach et al., 2007; Bush and Bambach, 2011; Bush et al., 2007).

16 Analysis of mammal diversity and hypotheses as to the processes that have shaped it tend to fall under a few categories: diversity of the whole system (Alroy, 1996; Alroy et al., 2000; Figueirido et al., 2012; Liow et al., 2008), guild based (Janis et al., 2000; Janis and Wilhelm, 1993; Jernvall and Fortelius, 2004; Pires et al., 2015; ?), clade based (Quental and Marshall, 2013; Slater, 2015),
18 climate based (Blois and Hadly, 2009; Janis, 1993; Janis and Wilhelm, 1993), and location based (Badgley and Finarelli, 2013; Eronen et al., 2015). Rarely are more than two of these categories
20 considered simultaneously, and instead integration of these diverse observations and hypotheses tends to be based on coincidence. The goal of this study is to pool information from multiple levels
22 of organization by integrating both species and climate data into a single analysis in order to provide a more holistic interpretation of the processes which may have shaped mammal species
24 diversity.

Fourth-corner modeling is an approach to explaining the patterns of either species abundance or
28 presence/absence as a product of species traits, environmental factors, and the interaction between
traits and environment (Brown et al., 2014; Jamil et al., 2013; Pollock et al., 2012; Warton et al.,
30 2015) CITATION. In modern ecological studies, what is being modeled is species occurrences at
localities distributed across a region (Jamil et al., 2013; Pollock et al., 2012). In this study, what is
32 being modeled is the pattern of species occurrence over time for most of the Cenozoic in North
America (Fig. 1). These two approaches, modern and paleontological, are different views of the same
34 three-dimensional pattern: species at localities over time. The temporal limitations of modern
ecological studies and difficulties with uneven spatial occurrences of fossils in paleontological studies
36 means that these approaches are complimentary but reveal different patterns of how species are
distributed in time and space.

38 One of the greatest challenges with analyzing species occurrence data is the inherent incompleteness
of any sample (Foote, 2001; Foote and Sepkoski, 1999; Lloyd et al., 2011; Royle and Dorazio, 2008;
40 Royle et al., 2014; Wang and Marshall, 2016). In the modern, only presences are certain as an
absence can be caused by both the species being truly absent or the species never having been
42 sampled (Royle and Dorazio, 2008; Royle et al., 2014). For paleontological data in the context of
this study, the incomplete preservation of fossil communities combined with the incomplete
44 sampling of what fossils there are means that the true times of origination or extinction may not be
observed (Foote, 2001; Foote and Sepkoski, 1999; Wang et al., 2016; Wang and Marshall, 2016).

46 In the analyses done here, a few key covariates which describe species' macroecology and
environmental context are considered. Because of the complexity of fourth-corner analyses in terms
48 of both number of covariates considered and structure of each model, it is possible to consider and
test a large number of possible hypotheses. Presented here are the species traits and related
50 hypotheses, followed by the environmental factors and related hypotheses.

The principle species trait considered in this study is a species' ecotype, defined here as the unique
52 combination of species dietary category and locomotor category (e.g. arboreal omnivore versus
unguligrade herbivore). This classification is analogous to the marine invertebrate ecocube discussed

- 54 above (Bush and Bambach, 2011; Bush et al., 2007; ?). Species mass was also included as a species trait, but is mostly included in order to control for that effect on species observation and occurrence.
- 56 Smits (2015) found several systematic differences in mammal species durations associated with various species traits. Omnivorous taxa were found to have, on average, a greater duration than
- 58 other dietary categories. Additionally, arboreal taxa were found to have a shorter duration than other locomotor categories.
- 60 An unresolved question from Smits (2015) is whether the greater extinction risk faced by arboreal is constant over time or if there was a change in extinction risk at the Paleogene/Neogene boundary.
- 62 Specifically, the question is whether the extinction risk arboreal taxa increased in the Neogene, driving the loss of arboreal taxa and average extinction risk of arboreal taxa down.
- 64 There are no observed massive cross-taxonomic turnover events in the North American record, unlike the Neogene record Europe (Alroy, 1996, 2009; Alroy et al., 2000; Eronen et al., 2015; ?).
- 66 The environmental factors included in this study include estimates of global temperature and the changing floral groups present in North America across the Cenozoic. Why are these factors
- 68 important? What are the hypotheses associated with environmental context?

Importantly, the probability of a species ecotype being present was modeled as a function of

70 environmental factors (Fig. 1).

The effect of climate on diversity and the diversification process has been the focus of considerable

72 research with many analyses favoring diversification being more biologically-mediated than

74 climate-mediated (Alroy, 1996; Alroy et al., 2000; Clyde and Gingerich, 1998; Figueirido et al.,

76 2012). Scale of analysis makes a big difference in interpretation of results, both temporal and

78 geographic. For example when the mammal fossil record analyzed at small temporal and geographic

80 scales a correlation between diversity and climate are observable (Clyde and Gingerich, 1998). However, when the record is analyzed at the scale of the continent and the Cenozoic there is no

82 correlation with diversity and climate (Alroy et al., 2000). This result, however, does not go

84 against the idea that there may be short periods of correlation and that this correlation changes or

80 reverse direction over time; instead this result means that there is no single direction of correlation
between diversity and climate (Figueirido et al., 2012).

82 In the case of a fluctuating correlation between diversity and climate it is hard to make the
argument of an actual causal link between the two without understanding the ecological differences
84 in mammalian fauna over time; when this analysis is based on diversity or taxonomy alone no
mechanisms are possible to infer. After all, taxonomy conflates many potential factors that could
86 affect diversification into a single variable; by separating the effects of shared common ancestry (i.e.
phylogeny) from species ecology the subtle differences in the diversification process can be observed
88 (Smits, 2015).

There are many candidate climatic events that may have influenced the distribution of mammal
90 ecotypes regionally, if not globally (Blois and Hadly, 2009; Zachos et al., 2008, 2001; ?). The
Paleocene-Eocene Temermal Maximum is associated with species dwarfing and rearrangement of
92 local communities, though regional effects are less known CITATION. The Mid-Miocene climactic
optimum is associated with WHAT CITATION. The

94 The general cooling throughout the Cenozoic and the development of ice-caps in the Neogene. The
Oligo-Miocene boundary.

96 One of the most stunning environmental transitions of the Cenozoic in North America was gradual
“opening-up” of the landscape with the shift from closed or partially forested environments of the
98 Paleogene to the savannah and grasslands environments that characterize the Neogene (Blois and
Hadly, 2009; Janis et al., 2000; Strömberg, 2005; ?).

100 Ultimately, the goal of this analysis are to understand when are unique ecotypes enriched or
depleted in the North American mammal regional species pool and how changes in ecotypic
102 diversity are related to changes in species' environmental context.

Materials and Methods

¹⁰⁴ Taxon occurrences and species-level information

All fossil occurrence information was downloaded from the Paleobiology Database.

¹⁰⁶ Occurrences (PBDB) were restricted to all Mammalia sampled in North America between the
Maastrichtian and Gelasian stages. Taxonomic, stratigraphic, and ecological metadata for each
¹⁰⁸ occurrence was included. The raw data is available for download at <http://goo.gl/2s1geU>.

This raw data was then sorted, cleaned, and manipulated programmatically prior to analysis.

¹¹⁰ Species taxonomic assignments given by the PBDB were updated for accuracy and consistency. For
example, species classified in the order Artiodactyla were reclassified as Cetartiodactyla. These
¹¹² re-assignments follow Smits (2015) and were Janis et al. (2008, 1998) and the Encyclopedia of Life
WEBSITE. Additionally, Taxa who's life habit was classified as either volant (i.e. Chiroptera) or
¹¹⁴ aquatic (e.g. Cetacea) were excluded from this analysis because of both differences in fossilization
potential and applicability to the study of terrestrial species pools.

¹¹⁶ The life habit and dietary categories provided through the PBDB were coarsened to increase per
ecotype sample size; this coarsening follows the same procedure as Smits (2015). Additionally, life
¹¹⁸ habit category was further modified to break-up the vague “ground-dwelling” category;
re-classifying these species by ankle posture gives more precise information about that species’
¹²⁰ environmental context. Ground-dwelling taxa were reassigned following ? by species taxonomic
context. Species ecotype is defined as the interaction between life habit and diet categories. Ecotype
¹²² categories with less than 10 species having ever been in that combination were excluded, yielding a
total of 18 of 24 possible ecotypes.

Table 2: Posture assignment based on taxonomy

Order	Family	Stance
	Ailuridae	plantigrade
	Allomyidae	plantigrade

Continued on next page

Table 2 – continued from previous page

Order	Family	Stance
	Amphicyonidae	plantigrade
	Amphilemuridae	plantigrade
	Anthracotheriidae	digitigrade
	Antilocapridae	unguligrade
	Apheliscidae	plantigrade
	Aplodontidae	plantigrade
	Apternodontidae	scansorial
	Arctocyonidae	unguligrade
	Barbourofelidae	digitigrade
	Barylambdidae	plantigrade
	Bovidae	unguligrade
	Camelidae	unguligrade
	Canidae	digitigrade
	Cervidae	unguligrade
	Cimolodontidae	scansorial
	Coryphodontidae	plantigrade
	Cricetidae	plantigrade
	Cylindrodontidae	plantigrade
	Cyriacotheriidae	plantigrade
	Dichobunidae	unguligrade
Dinocerata		unguligrade
	Dipodidae	digitigrade
	Elephantidae	digitigrade
	Entelodontidae	unguligrade
	Eomyidae	plantigrade

Continued on next page

Table 2 – continued from previous page

Order	Family	Stance
	Erethizontidae	plantigrade
	Erinaceidae	plantigrade
	Esthonychidae	plantigrade
	Eutypomyidae	plantigrade
	Felidae	digitigrade
	Florentiamyidae	plantigrade
	Gelocidae	unguligrade
	Geolabididae	plantigrade
	Glyptodontidae	plantigrade
	Gomphotheriidae	unguligrade
	Hapalodectidae	plantigrade
	Heteromyidae	digitigrade
	Hyaenidae	digitigrade
	Hyaenodontidae	digitigrade
	Hypertragulidae	unguligrade
	Ischyromyidae	plantigrade
	Jimomyidae	plantigrade
Lagomorpha		digitigrade
	Leptictidae	plantigrade
	Leptochoeridae	unguligrade
	Leptomerycidae	unguligrade
	Mammutidae	unguligrade
	Megalonychidae	plantigrade
	Megatheriidae	plantigrade
	Mephitidae	plantigrade

Continued on next page

Table 2 – continued from previous page

Order	Family	Stance
	Merycoidodontidae	digitigrade
Mesonychia		unguligrade
	Mesonychidae	digitigrade
	Micropternodontidae	plantigrade
	Mixodectidae	plantigrade
	Moschidae	unguligrade
	Muridae	plantigrade
	Mustelidae	plantigrade
	Mylagaulidae	fossorial
	Mylodontidae	plantigrade
	Nimravidae	digitigrade
	Nothrotheriidae	plantigrade
Notoungulata		unguligrade
	Oromerycidae	unguligrade
	Oxyaenidae	digitigrade
	Palaeomerycidae	unguligrade
	Palaeoryctidae	plantigrade
	Pampatheriidae	plantigrade
	Pantolambdidae	plantigrade
	Periptychidae	digitigrade
Perissodactyla		unguligrade
	Phenacodontidae	unguligrade
Primates		plantigrade
	Procyonidae	plantigrade
	Proscalopidae	plantigrade

Continued on next page

Table 2 – continued from previous page

Order	Family	Stance
	Protoceratidae	unguligrade
	Reithroparamyidae	plantigrade
	Sciuravidae	plantigrade
	Sciuridae	plantigrade
	Simimyidae	plantigrade
	Soricidae	plantigrade
	Suidae	digitigrade
	Talpidae	fossorial
	Tayassuidae	unguligrade
	Tenrecidae	plantigrade
	Titanoideidae	plantigrade
	Ursidae	plantigrade
	Viverravidae	plantigrade
	Zapodidae	plantigrade

124

Species mass information was gathered from multiple different sources where a plurality of the body size estimates are from the PBDB. Body part measurements for many species are also available through the PBDB. Just as with Smits (2015), these measurements and corresponding regression equations were used to get mass estimates for more species. Additional mass estimates and body part measurements were sourced from numerous publications and the Neogene Old World Database; see the supplementary material to Smits (2015) for details. Mass was log-transformed and then mean-centered and rescaled by dividing by two-times its standard deviation; this insures that the magnitude of effects for both continuous and discrete covariates are comparable (Gelman, 2008; Gelman and Hill, 2007).

Table 1: Species trait assignments in this study are a coarser version of the information available in the PBDB. Information was coarsened to improve per category sample size and uniformity and followed this table.

This study		PBDB categories
Diet	Carnivore	Carnivore
	Herbivore	Browser, folivore, granivore, grazer, herbivore.
	Insectivore	Insectivore.
	Omnivore	Frugivore, omnivore.
Locomotor	Arboreal	Arboreal.
	Ground dwelling	Fossorial, ground dwelling, semifossorial, saltatorial.
	Scansorial	Scansorial.

- ¹³⁴ All fossil occurrences from 64 to 2 million years ago (Mya) were binned into 31 2 million year (My) bins. This temporal length was chosen because it is approximately the resolution of the North
¹³⁶ American mammal fossil record.

Environmental and temporal covariates

- ¹³⁸ The group-level covariates in this study are descriptors of species' environmental context, specifically global temperature estimates and Graham's floral intervals CITATION. Global
¹⁴⁰ temperature across most of the Cenozoic was calculated from Mg/Ca isotope record from deep sea carbonates (Cramer et al., 2011). Mg/Ca based temperature estimates are preferable to the
¹⁴² frequently used $\delta^{18}\text{O}$ temperature proxy (Alroy et al., 2000; Figueirido et al., 2012; Zachos et al., 2008, 2001) because Mg/Ca estimates do not conflate temperature with ice sheet volume and
¹⁴⁴ depth/stratification changes; this makes it preferable as an estimate of global temperature for macroevolutionary and macroecological studies (Ezard et al., 2016).
¹⁴⁶ Two aspects of the Mg/Ca-based temperature curve were included in this analysis: mean and range. Both were calculated as the mean of all respective estimates for each 2 My temporal bins. Both
¹⁴⁸ mean and range were then rescaled as above: subtract mean, divide by twice the standard deviation.
The other major set of environmental factors included in this study are Graham's Cenozoic plant
¹⁵⁰ phases CITATION. Graham's plant phases are holistic descriptors of the taxonomic composition of which plants were present at a given time and their relative modernity, with younger phases

Table 3: Regression equations used in this study for estimating body size. Equations are presented with reference to taxonomic grouping, part name, and reference.

Group	Equation	log(Measurement)	Source
General	$\log(m) = 1.827x + 1.81$	lower m1 area	Legendre (1986)
General	$\log(m) = 2.9677x - 5.6712$	mandible length	?
General	$\log(m) = 3.68x - 3.83$	skull length	?
Carnivores	$\log(m) = 2.97x + 1.681$	lower m1 length	?
Insectivores	$\log(m) = 1.628x + 1.726$	lower m1 area	?
Insectivores	$\log(m) = 1.714x + 0.886$	upper M1 area	?
Lagomorph	$\log(m) = 2.671x - 2.671$	lower toothrow area	Tomiya (2013)
Lagomorph	$\log(m) = 4.468x - 3.002$	lower m1 length	Tomiya (2013)
Marsupials	$\log(m) = 3.284x + 1.83$	upper M1 length	?
Marsupials	$\log(m) = 1.733x + 1.571$	upper M1 area	?
Rodentia	$\log(m) = 1.767x + 2.172$	lower m1 area	Legendre (1986)
Ungulates	$\log(m) = 1.516x + 3.757$	lower m1 area	?
Ungulates	$\log(m) = 3.076x + 2.366$	lower m2 length	?
Ungulates	$\log(m) = 1.518x + 2.792$	lower m2 area	?
Ungulates	$\log(m) = 3.113x - 1.374$	lower toothrow length	?

- 152 representing increasingly modern taxa CITATION. Graham CITATION defines four intervals from
the Cretaceous to the Pliocene, though only three of these intervals are included in this analysis.
154 Graham’s plant phases CITATION was included as a series of “dummy variables” encoding the
three phases included in this analysis. This means that the first phase is synonymous with the
156 intercept and phases

Modelling species occurrence

- 158 Two different models were used in this study: a pure-presence model and a birth-death model. Both
models at their core are hidden Markov model where the latent aspect of the process has an
160 absorbing state (Allen, 2011). The difference between these two models is if the probability of a
species origination and survival are considered equal or different (Table 4). Something that is
162 important to realize is that while there are only two state “codes” in a presence-absence matrix (i.e.
0/1), there are in fact three states in a birth-death model: never having originated, extant, and
164 extinct. The last of these is the absorbing state, as once a species has gone extinct it cannot
re-originate (Allen, 2011); this is made obvious in the transition matrices as the probability of an

		State at $t + 1$		
		0_{never}	1	$0_{extinct}$
State at t	0_{never}	$1 - \theta$	θ	0
	1	0	θ	$1 - \theta$
	$0_{extinct}$	0	0	1

(a) Pure-presence

		State at $t + 1$		
		0_{never}	1	$0_{extinct}$
State at t	0_{never}	$1 - \phi$	ϕ	0
	1	0	π	$1 - \pi$
	$0_{extinct}$	0	0	1

(b) Birth-death

Table 4: Transition matrices for the pure-presence (4a) and birth-death (4b) models. Both of these models share the core machinery of discrete-time birth-death processes but make distinct assumptions about the equality of originating and surviving (Eq. 2, and 3). Note also that while there are only two state “codes” (0, 1), there are in fact three states: never having originated 0_{never} , present 1, extinct $0_{extinct}$ (Allen, 2011).

¹⁶⁶ extinct species changing states is 0 (Table 4). See below for parameter explainations (Tables 6, and 7).

¹⁶⁸ Data augmentation

All presence/absence observations are incomplete. The hidden Markov model at the core of this ¹⁷⁰ analysis allows for observed absences to be used meaningfully to estimate the number of unobserved species. Of specific concern in this analysis is the unknown “true” size of the dataset; how many ¹⁷² species could have actually been observed? While many species have been observed, the natural incompleteness of all observations, especially in the case of paleontological data, there are obviously ¹⁷⁴ many species which were never sampled (Royle and Dorazio, 2008; Royle et al., 2007).

Let N by the total number of observed species, M be the upper limit of possible species that could ¹⁷⁶ have existed given a model of species presence, and N^* is the all-zero histories where $N^* = M - N$. This approach assumes that $\hat{N} \sim \text{Binomial}(M, \psi)$ where \hat{N} is the estimated “true” number of ¹⁷⁸ species and ψ is the probability that any augmented species should actually be “present.” Because M is user defined, this approach effectively gives ψ a uniform prior over N to M (Royle and ¹⁸⁰ Dorazio, 2008). For this study, $M = N + [N/4]$.

Data imputation is the process of estimating missing data for partially observed covariates (Gelman ¹⁸² and Hill, 2007; Rubin, 1996), this is simple in a Bayesian context because data are also parameters (Gelman et al., 2013). Augmented species also have no known mass so a mass estimate must be

184 imputed for each possible species (Royle and Dorazio, 2012). This procedure assumes that mass
 values for augmented species are from the same distribution as observed species. The distribution of
 186 observed mass values is estimated as part of the model, and new mass values are then generated
 from this distribution. This approach is an example of imputing data missing completely at random
 188 (Gelman and Hill, 2007; Royle and Dorazio, 2012). Because log mass values are rescaled as a part of
 this study, the body mass distribution is already known ($\mathcal{N}(0, 0.5)$); augmented species body mass
 190 just simply drawn from this distribution.

In addition to body mass information, the augmented species need an ecotype classification. Because
 192 these species are completely unknown, they were all classified as “augmented,” an additional
 grouping indicating their unknown biology. This classification has no biological interpretation.

194 **Observation process**

The type of hidden Markov model used in this study has three characteristic probabilities:
 196 probability p of observing a species given that it is present, probability ϕ of a species surviving from
 one time to another, and probability π of a species first appearing (Royle and Dorazio, 2008). In
 198 this formulation, the probability of a species going extinct is $1 - \pi$. For the pure-presence model
 $\phi = \pi$, while for the birth-death model $\phi \neq \pi$.
 200 The probability of observing a species that is present p is modeled as a logistic regression was a
 time-varying intercept and species mass as a covariate. The effect of species mass on p was assumed
 202 linear and constant over time and given a prior reflecting a possible positive relationship; these
 assumptions are reflected in the structure of the model Equation 1. The parameters associated with
 204 this part of the model are described in Table 5.

$$\begin{aligned}
 y_{i,t} &\sim \text{Bernoulli}(p_{i,t} z_{i,t}) \\
 p_{i,t} &= \text{logit}^{-1}(\alpha_0 + \alpha_1 m_i + r_t) \\
 r_t &\sim \mathcal{N}(0, \sigma)
 \end{aligned} \tag{1}$$

Table 5: Observation parameters

Parameter	dimensions	explanation
y	$N \times T$	observed species presence/absence
z	$N \times T$	“true” species presence/absence
p	T	probability of observing a species that is present at time t
m	N	species log mass, rescaled
α_0	1	average log-odds of p
α_1	1	change in average log-odds of p per change mass
r	T	difference from α_0 associated with time t
σ	1	standard deviation of r

Table 6: Parameters for the model of presence in the pure-presence model

Parameter	dimensions	explanation
z	$N \times T$	“true” species presence/absence
θ	$N \times T - 1$	probability of $z = 1$
a	$T - 1 \times D$	ecotype-varying intercept; mean value of log-odds of θ
m	N	species log mass, rescaled
b_1	1	effect of species mass on log-odds of θ
b_2	1	effect of species mass, squared, on log-odds of θ
U	$T \times D$	matrix of group-level covariates
γ	$U \times D$	matrix of group-level regression coefficients
Σ	$D \times D$	covariance matrix of a
Ω	$D \times D$	correlation matrix of a
τ	D	vector of standard deviations for each ecotype a_d

Pure-presence process

- 206 For the pure-presence model there is only a single probability dealing with the presence of a species
 θ (Table 4a). This probability was modeled as multi-level logistic regression with both species-level
208 and group-level covariates (Gelman et al., 2013; Gelman and Hill, 2007). The parameters associated
with pure-presence model are presented in Table 6 and the full sampling statement in Equation 2.
- 210 The species-level of the model (Eq. 2) is a logistic regression with varying-intercept that varies by
ecotype. Additionally, species mass was included as a covariate associated with two regression
212 coefficients allowing a quadratic relationship with log-odds of occurrence. This assumption is based
on the known distribution of mammal body masses where species with intermediate mass values are
214 more common than either small or large bodied species. These assumptions are also reflected in the
choice of priors for these regression coefficients.

216 The values of each ecotype's intercept are themselves modeled as regressions using the group-level
 covariates associated with environmental context. Each of these regressions has an associated
 218 variance of possible values of each ecotype's intercept (Gelman and Hill, 2007). In addition, the
 covariances between ecotype intercepts, given this group-level regression, are modeled (Gelman and
 220 Hill, 2007).

All parameters not modeled elsewhere were given weakly informative priors (Gelman et al., 2013)
 222 CITATION STAN MANUAL STATISTICAL RETHINKING. Weakly informative means that
 priors do not necessarily encode actual prior information but instead help regularize or weakly
 224 constrain posterior estimates. These priors have a concentrated probability density around and near
 zero; this has the effect of tempering our estimates and help prevent overfitting the model to the
 226 data (Gelman et al., 2013) CITATION STAN MANUAL STATISTICAl RETHINKING.

$$\begin{aligned}
 y_{i,t} &\sim \text{Bernoulli}(p_{i,t} z_{i,t}) & \alpha_0 &\sim \mathcal{N}(0, 1) \\
 p_{i,t} &= \text{logit}^{-1}(\alpha_0 + \alpha_1 m_i + r_t) & \alpha_1 &\sim \mathcal{N}(1, 1) \\
 r_t &\sim \mathcal{N}(0, \sigma) & \sigma &\sim \mathcal{N}^+(1) \\
 z_{i,1} &\sim \text{Bernoulli}(\rho) & b_1 &\sim \mathcal{N}(0, 1) \\
 z_{i,t} &\sim \text{Bernoulli}(\theta_{i,t}) & b_2 &\sim \mathcal{N}(-1, 1) \\
 \theta_{i,t} &= \text{logit}^{-1}(a_{t,j[i]} + b_1 m_i + b_2 m_i^2) & \gamma &\sim \mathcal{N}(0, 1) \\
 a &\sim \text{MVN}(u\gamma, \Sigma) & \tau &\sim \mathcal{N}^+(1) \\
 \Sigma &= \text{diag}(\tau)\Omega\text{diag}(\tau) & \Omega &\sim \text{LKJ}(2)
 \end{aligned} \tag{2}$$

Birth-death process

228 In the birth-death model, $\phi \neq \pi$ and so each of these probabilities are modeled separately but in a
 similar manner to how θ is modeled in the pure-presence model (Eq. 2, Table 4b). The parameters
 230 associated with the birth-death presence model are presented in Table 7 and the full sampling
 statement, including observation (Eq. 1), is described in Equation 3.

Table 7: Parameters for the model of presence in the pure-presence model

Parameter	dimensions	explanation
z	$N \times T$	“true” species presence/absence
ϕ	$N \times T$	probability of $z_{-,t} = 1 z_{-,t-1} = 0$
π	$N \times T - 1$	probability of $z_{-,t} = 1 z_{-,t-1} = 1$
a^ϕ	$T - 1 \times D$	ecotype-varying intercept; mean value of log-odds of θ
a^π	$T - 1 \times D$	ecotype-varying intercept; mean value of log-odds of θ
m	N	species log mass, rescaled
b_1^ϕ	1	effect of species mass on log-odds of ϕ
b_1^π	1	effect of species mass on log-odds of π
b_2^ϕ	1	effect of species mass, squared, on log-odds of ϕ
b_2^π	1	effect of species mass, squared, on log-odds of π
U	$T \times D$	matrix of group-level covariates
γ^ϕ	$U \times D$	matrix of group-level regression coefficients
γ^π	$U \times D$	matrix of group-level regression coefficients
Σ^ϕ	$D \times D$	covariance matrix of a^ϕ
Σ^π	$D \times D$	covariance matrix of a^π
Ω^ϕ	$D \times D$	correlation matrix of a^ϕ
Ω^π	$D \times D$	correlation matrix of a^π
τ^ϕ	D	vector of standard deviations for each ecotype a_d^ϕ
τ^π	D	vector of standard deviations for each ecotype a_d^π

- ²³² Similar to the pure-presence model, both ϕ and π are modeled as logistic regressions with varying-intercept and one covariate associated with two parameters. The possible relationships between mass and both ϕ and π are reflected in the parameterization of the model and choice of priors (Eq. 3).
- ²³⁴ The intercepts of ϕ and π both vary by species ecotype and those values are themselves the product of group-level regression using environmental factors as covariates (Eq. 3); this is identical to the

²³⁸ pure presence model (Eq. 2).

$$\begin{aligned}
y_{i,t} &\sim \text{Bernoulli}(p_{i,t} z_{i,t}) & \Sigma^\phi &= \text{diag}(\tau^\phi) \Omega^\phi \text{diag}(\tau^\phi) \\
p_{i,t} &= \text{logit}^{-1}(\alpha_0 + \alpha_1 m_i + r_t) & \Sigma^\pi &= \text{diag}(\tau^\pi) \Omega^\pi \text{diag}(\tau^\pi) \\
r_t &\sim \mathcal{N}(0, \sigma) & \rho &\sim U(0, 1) \\
\alpha_0 &\sim \mathcal{N}(0, 1) & b_1^\phi &\sim \mathcal{N}(0, 1) \\
\alpha_1 &\sim \mathcal{N}(1, 1) & b_1^\pi &\sim \mathcal{N}(0, 1) \\
\sigma &\sim \mathcal{N}^+(1) & b_2^\phi &\sim \mathcal{N}(-1, 1) \\
z_{i,1} &\sim \text{Bernoulli}(\phi_{i,1}) & b_2^\pi &\sim \mathcal{N}(-1, 1) \\
z_{i,t} &\sim \text{Bernoulli} \left(z_{i,t-1} \pi_{i,t} + \sum_{x=1}^t (1 - z_{i,x}) \phi_{i,t} \right) & \gamma^\phi &\sim \mathcal{N}(0, 1) \\
&& \gamma^\pi &\sim \mathcal{N}(0, 1) \\
\phi_{i,t} &= \text{logit}^{-1}(a_{t,j[i]}^\phi + b_1^\phi m_i + b_2^\phi m_i^2) & \tau^\phi &\sim \mathcal{N}^+(1) \\
\pi_{i,t} &= \text{logit}^{-1}(a_{t,j[i]}^\pi + b_1^\pi m_i + b_2^\pi m_i^2) & \tau^\pi &\sim \mathcal{N}^+(1) \\
a^\phi &\sim \text{MVN}(U \gamma^\phi, \Sigma^\phi) & \Omega^\phi &\sim \text{LKJ}(2) \\
a^\pi &\sim \text{MVN}(U \gamma^\pi, \Sigma^\pi) & \Omega^\pi &\sim \text{LKJ}(2)
\end{aligned} \tag{3}$$

Posterior inference and model adequacy

²⁴⁰ Programs that implement joint posterior inference for the above models (Eqs. 2, 3) were
 implemented in the probabilistic programming language Stan CITATION. The models used here
²⁴² both feature latent discrete parameters in the large matrix z (Tables 5, 6, 7; Eqs. 1, 2, 3). All
 methods for posterior inference implemented in Stan are derivative based which causes
²⁴⁴ complications for actually implementing the above models because integers do not have derivatives.
 Instead of implementing a latent discrete parameterization, the posterior probabilities of all possible
²⁴⁶ states of the latent parameters z were estimated (i.e. marginalized).

Species durations at minimum range-through from the FAD to the LAD, but the incompleteness of

248 all observations means that the actual time of origination or extinction is unknown. The
marginalization approach used here means that the probabilities all possible histories for a species
250 are calculated, from the end members of the species having existed for the entire study interval and
the species having only existed between the directly observed FAD and LAD to all possible
252 intermediaries CITATION STAN MANUAL.

The combined size of the dataset and large number of parameters in both models (Eqs. 2, 3),
254 specifically the total number of latent parameters that are the matrix z , means that stochastic
approximate posterior inference is computationally very slow even using HMC. Instead, an
256 approximate Bayesian approach was used: variational inference. A recently developed automatic
variational inference algorithm called “automatic differentiation variational inference” (ADVI) is
258 implemented in Stan and was used here CITATION. ADVI assumes that the posterior is Gaussian
but still yields a true Bayesian posterior; this assumption is similar to quadratic approximation of
260 the likelihood function used in maximum likelihood inference CITATION. The principal limitation
of assuming the joint posterior is Gaussian is that the true topology of the log-posterior isn’t
262 estimated; this is a particular burden for scale parameters which are bound to be positive (e.g.
standard deviation).

264 After fitting both models (Eqs. 2, 3) using ADVI, model adequacy and quality of fit was assessed
using a series of posterior predictive checks CITATION CITATION. Because all Bayesian models
266 are inherently generative, simulations of new data sets is “free” CITATION. By simulating many
theoretical data sets using the observed covariate information the congruence between predictions
268 made by the model and the observed empirical data can be assessed. By combining multiple
posterior predictive tests of congruence between empirical and simulated values of interest, the
270 holistic adequacy of the model can be analyzed CITATION.

An example posterior predictive check used in this study was comparing the observed average
272 number of observations per species to a distribution of simulated averages; if the empirically
observed value sits in the middle of the distribution than the model is adequate in reproducing the
274 observed number of occurrences per species.

Posterior simulations for time series are start with the values at $t = 1$ and then just simulating
 276 forward.

Given parameter estimates, diversity and diversification rates are estimated through posterior
 278 predictive simulations. Given the observed presence-absence matrix y , estimates of the true
 presence-absence matrix z can be simulated and the distribution of possible occurrence histories
 280 can be analyzed. This is conceptually similar to marginalization where the probability of each
 possible occurrence history is estimated (Fig. 2).

282 The posterior distribution of z gives the estimate of standing diversity N_t^{stand} for all time points as

$$N_t^{stand} = \sum_{i=1}^M z_{i,t}. \quad (4)$$

Given estimates of N^{stand} for all time points, the estimated number of originations O_t are be
 284 estimated as

$$O_t = \sum_{i=1}^M z_{i,t} = 1 | z_{i,t-1} = 0 \quad (5)$$

and number of extinctions E_t estimated as

$$E_t = \sum_{i=1}^M z_{i,t} = 0 | z_{i,t-1} = 1. \quad (6)$$

286 Per-captia growth D^{rate} , origination O^{rate} and extinction E^{rate} rates are then calculated as

$$\begin{aligned} O_t^{rate} &= \frac{O_t}{N_{t-1}^{stand}} \\ E_t^{rate} &= \frac{E_t}{N_{t-1}^{stand}} \\ D_t^{rate} &= O_t^{rate} - E_t^{rate}. \end{aligned} \quad (7)$$

Results

288 Posterior results take one of two forms: direct inspection of parameter estimates, and downstream
estimates of diversity and diversification rates. For the former, both the pure-presence and
290 birth-death models (Eq. 2, and 3 are inspected. For the latter, only posterior estimates from the
birth-death model are considered; the reason for this is explained below in the comparison of the
292 models' posterior predictive check results.

Comparing parameter estimates from the pure-presence and birth-death models

Comparison of the posterior predictive performance of the pure-presence and birth-death models
296 reveals a striking difference in quality of the models' fits to the data (Fig. 3a and 3b). The
birth-death model is clearly able to reproduce the observed average number of occurrence, in
298 contrast to the pure-birth model which greatly underestimates the ovserved average number of
occurrences. The interpretation of these results is that the results of the birth-death model are
300 more representative of the data than the pure-presence model, though further inspection of the
posterior parameter estimates can provide further insight into why these models give different
302 posterior predictive results (Gelman et al., 2013). However, it is expected that downstream analyses
from the birth-death model will be more reliable than that from the pure-presence model.

304 Occurrence probabilities estimated from the pure-presence model (Fig. 4) are much more similar to
the origination estimates from the birth-death model (Fig. 5) than the estimates of survival
306 probability (Fig. 6).

In general, both occurrence probabilities estimated from the pure-presence model (Fig. 4) and
308 origination probabilities estimated from the birth-death model (fig. 5) increase with time. Notable,
ecotypes with arboreal components do not follow this average; instead, occurrence and origination
310 probabilities appear relatively flat for most of the Cenozoic.

The dramatic differences between origination and survival probabilities indicate how different these

312 processes are, and may be responsible for the better posterior predictive performance of the
birth-death model over the pure-presence model (Fig. 3a, and 3b). While the estimates of both time
314 series have high variance, what is striking is how mean origination probability changes over time
while in general survival probabilities have relatively stable means (Fig. 5, and 6).

316 Estimates of origination probabilities appear to have less uncertainty than for survival (Fig. 5, and
6).

318 The pure-presence and birth-death models differ in estimated effect of mass on the probability of
observing a species that is present (Fig. 7). For the pure-presence model, mass is estimated to have
320 no effect on the probability of observing a species that is present (Fig. 7a). Contrastingly, for the
birth-death model mass is found to have a negative relationship with observation such that larger
322 species are less likely to be observed if present than smaller species (Fig. 7b).

The result from the birth-death model is unexpected given that it is generally assumed that larger
324 mammals are more likely to have been collected than smaller mammals CITATION. However,
collection is not preservation; similarities in preservation rate indicate similarities in how gap-filled
326 species records are. What this result means is that the record of large bodied species is expected on
average to be more gap-filled and less consistent from time point to time point than smaller bodied
328 species. Additionally, this is presence/absence data, so higher preservation and collection in terms
of individual specimens at a location or a single temporal horizon does not necessarily translate to
330 high preservation over time.

The effect of species mass on probability of occurrence as estimated from the pure-presence (Fig. 8)
332 is most similar to the effect of species mass on probability of origination as estimates from the
birth-death model (Fig. 9). The striking pattern observable in both sets of estimates is the higher
334 probability of occurrence for species with body sizes closer to the mean than either extremes. This
result is consistent with the canonically normal distribution of mammal body sizes CITATION; it is
336 then expected that the most likely to occur species would be those from the middle of the
distribution, and that species originating will on average be of average mass, especially considering
338 species shared common ancestry CITATION.

In contrast, the effect of species mass on probability of survival as estimated from the birth-death
340 model (Fig. 10) indicates little effect of mass on extinction; this is consistent with previous findings
from the North American mammal fossil record (Smits, 2015; Tomiya, 2013). Note that all variation
342 between ecotypes is due to differences in ecotype-specific survival probability and the associated
effects of plant phase.

344 Similarities in parameters estimates between ecotypes may be due to similar response to
environmental factors. Some of the obvious patterns from inspection of the individual-level
346 estimates of occurrence (Fig. 4), origination (Fig. 5), and survival probabilities (Fig. 6) that are of
note are the similarities between arboreal taxa and the differences between arboreal and all other
348 taxa.

Inspection of parameter estimates for the group-level covariates

350 **Analysis of diversity**

All analyses of diversification and macroevolutionary rates has been done using only the birth-death
352 model; this is because of the models better posterior predictive check performance (Fig. 3a, and 3b).

For the first half of the Cenozoic there appears to be a very slow decline and then plateau in total
354 diversity until the WHEN? (Fig. 14a).

When viewed through the lens of diversification rate the structure behind this pattern begins to
356 take shape (Fig. 14b). For approximately the first third of the Cenozoic, diversification rate is
frequently below zero species gained per species present per two million years; this is broken up by
358 few inferred spikes in diversification WHEN?. During the observed period of possible stability in

The comparison between per capita origination and extinction rate estimates reveals how
360 diversification rate is formed (Fig. 14c, 14d). Origination rate seems most closely mimic
diversification rate while extinction rate has a saw-toothed pattern for the Cenozoic with no
362 obvious emergent structure; inferred spikes in origination rate do not correspond to any spikes in
extinction rate.

- ³⁶⁴ Diversity partitioned by ecotype reveals a lot of the complexity behind the pattern of mammal diversity for the Cenozoic (Fig. 15).
- ³⁶⁶ An impressive commonality across multiple ecotype-specific diversity time series are two spikes in diversity, either up or down (Fig. 15). Spikes of increased diversity are seen this is seen in all arboreal ecotypes, plantigrade insectivores, scansorial insectivores, and scansorial omnivores. The converse pattern, spikes of decreased diversity, are strongly observed in the diversity history of digitigrade herbivores, with weaker decreases observed in the histories of digitigrade carnivores, and unguiligrade herbivores.
- ³⁷² Arboreal ecotypes are estimated to have disappeared and reappeared as short bursts over the last 65 million years in North America, with arboreal carnivores and insectivores being most often rarer than arboreal herbivores and omnivores.
- ³⁷⁴

Fossorial ecotypes, whether herbivorous and insectivorous appear rare or possibly absent for most of the Cenozoic, which maximum estimated diversity being obtained in the latter half of the time series (Fig. 15).

³⁷⁸ Plantigrade ecotypes appear most variable, plantigrade herbivores having a very different diversity history than plantigrade carnivores and omnivores and plantigrade insectivores.

³⁸⁰ Unguligrade and plantigrade herbivores have relatively stable standing diversities throughout the Cenozoic of North America (Fig. 15). Similarly, digitigrade carnivorous taxa appear to have a relatively stable diversity for the Cenozoic.

³⁸²

Discussion

³⁸⁴ Acknowledgements

I would like to thank K. Angielczyk, M. Foote, P. D. Polly, and R. Ree for helpful discussion and advice. This entire study would not have been possible without the Herculean effort of the

many contributors to the Paleobiology Database. In particular, I would like to thank J. Alroy and
388 M. Uhen for curating most of the mammal occurrences recorded in the PBDB. This is Paleobiology
Database publication XXX.

390 **References**

- Allen, L. J. S. 2011. An introduction to stochastic processes with applications to biology. 2nd ed.
392 Chapman and Hall/CRC, Boca Raton, FL.
- Alroy, J. 1996. Constant extinction, constrained diversification, and uncoordinated stasis in North
394 American mammals. *Palaeogeography, Palaeoclimatology, Palaeoecology* 127:285–311.
- . 2009. Speciation and extinction in the fossil record of North American mammals. Pages
396 302–323 *in* R. K. Butlin, J. R. Bridle, and D. Schluter, eds. *Speciation and patterns of diversity*.
Cambridge University Press, Cambridge.
- 398 Alroy, J., P. L. Koch, and J. C. Zachos. 2000. Global climate change and North American
mammalian evolution. *Paleobiology* 26:259–288.
- 400 Badgley, C., and J. A. Finarelli. 2013. Diversity dynamics of mammals in relation to tectonic and
climatic history: comparison of three Neogene records from North America. *Paleobiology*
402 39:373–399.
- Bambach, R. K. 1977. Species richness in marine benthic habitats through the Phanerozoic.
404 *Paleobiology* 3:152–167.
- Bambach, R. K., A. M. Bush, and D. H. Erwin. 2007. Autecology and the filling of ecospace: Key
406 metazoan radiations. *Palaeontology* 50:1–22.
- Blois, J. L., and E. A. Hadly. 2009. Mammalian Response to Cenozoic Climatic Change. Annual
408 Review of Earth and Planetary Sciences 37:181–208.
- Brown, A. M., D. I. Warton, N. R. Andrew, M. Binns, G. Cassis, and H. Gibb. 2014. The

- 410 fourth-corner solution - using predictive models to understand how species traits interact with
the environment. *Methods in Ecology and Evolution* 5:344–352.
- 412 Bush, A. M., and R. K. Bambach. 2011. Paleoecologic Megatrends in Marine Metazoa, vol. 39.
Bush, A. M., R. K. Bambach, and G. M. Daley. 2007. Changes in theoretical ecospace utilization in
414 marine fossil assemblages between the mid-Paleozoic and late Cenozoic. *Paleobiology* 33:76–97.
- Clyde, W. C., and P. D. Gingerich. 1998. Mammalian community response to the latest Paleocene
416 thermal maximum: an isotaphonomic study in the northern Bighorn Basin, Wyoming. *Geology*
26:1011–1014.
- 418 Cramer, B. S., K. Miller, P. Barrett, and J. Wright. 2011. Late Cretaceous-Neogene trends in deep
ocean temperature and continental ice volume: Reconciling records of benthic foraminiferal
420 geochemistry ($\delta^{18}\text{O}$ and Mg/Ca) with sea level history. *Journal of Geophysical Research: Oceans*
116:1–23.
- 422 Eronen, J. T., C. M. Janis, C. P. Chamberlain, and A. Mulch. 2015. Mountain uplift explains
differences in Palaeogene patterns of mammalian evolution and extinction between North
424 America and Europe. *Proceedings of the Royal Society B: Biological Sciences* 282:20150136.
- Ezard, T. H. G., A. Purvis, and H. Morlon. 2016. Environmental changes define ecological limits to
426 species richness and reveal the mode of macroevolutionary competition. *Ecology Letters*
19:899–906.
- 428 Figueirido, B., C. M. Janis, J. A. Pérez-Claros, M. De Renzi, and P. Palmqvist. 2012. Cenozoic
climate change influences mammalian evolutionary dynamics. *Proceedings of the National
430 Academy of Sciences* 109:722–727.
- Foote, M. 2001. Inferring temporal patterns of preservation, origination, and extinction from
432 taxonomic survivorship analysis. *Paleobiology* 27:602–630.
- Foote, M., and J. J. Sepkoski. 1999. Absolute measures of the completeness of the fossil record.
434 *Nature* 398:415–7.

- Gelman, A. 2008. Scaling regression inputs by dividing by two standard deviations. Statistics in
436 Medicine pages 2865–2873.
- Gelman, A., J. B. Carlin, H. S. Stern, D. B. Dunson, A. Vehtari, and D. B. Rubin. 2013. Bayesian
438 data analysis. 3rd ed. Chapman and Hall, Boca Raton, FL.
- Gelman, A., and J. Hill. 2007. Data Analysis using Regression and Multilevel/Hierarchical Models.
440 Cambridge University Press, New York, NY.
- Jamil, T., W. A. Ozinga, M. Kleyer, and C. J. F. Ter Braak. 2013. Selecting traits that explain
442 species-environment relationships: A generalized linear mixed model approach. Journal of
Vegetation Science 24:988–1000.
- Janis, C. M. 1993. Tertiary mammal evolution in the context of changing climates, vegetation, and
tectonic events. Annual Review of Ecology and Systematics 24:467–500.
- 444 Janis, C. M., J. Damuth, and J. M. Theodor. 2000. Miocene ungulates and terrestrial primary
productivity: where have all the browsers gone? Proceedings of the National Academy of Sciences
448 97:7899–904.
- Janis, C. M., G. F. Gunnell, and M. D. Uhen. 2008. Evolution of Tertiary mammals of North
450 America. Vol. 2. Small mammals, xenarthrans, and marine mammals. Cambridge University
Press, Cambridge.
- 452 Janis, C. M., K. M. Scott, and L. L. Jacobs. 1998. Evolution of Tertiary mammals of North
America. Vol. 1. Terrestrial carnivores, ungulates, and ungulatelike mammals. Cambridge
454 University Press, Cambridge.
- Janis, C. M., and P. B. Wilhelm. 1993. Were there mammalian pursuit predators in the tertiary?
456 Dances with wolf avatars. Journal of Mammalian Evolution 1:103–125.
- Jernvall, J., and M. Fortelius. 2004. Maintenance of trophic structure in fossil mammal
458 communities: site occupancy and taxon resilience. The American Naturalist 164:614–624.

- Legendre, S. 1986. Analysis of mammalian communities from the Late Eocene and Oligocene of
460 Southern France. *Paleovertebrata* 16:191–212.
- Liow, L. H., M. Fortelius, E. Bingham, K. Lintulaakso, H. Mannila, L. Flynn, and N. C. Stenseth.
462 2008. Higher origination and extinction rates in larger mammals. *Proceedings of the National
Academy of Sciences* 105:6097–6102.
- 464 Lloyd, G. T., J. R. Young, and A. B. Smith. 2011. Taxonomic Structure of the Fossil Record is
Shaped by Sampling Bias. *Systematic Biology* 61:80–89.
- 466 Pires, M. M., D. Silvestro, and T. B. Quental. 2015. Continental faunal exchange and the
asymmetrical radiation of carnivores. *Proceedings of the Royal Society B: Biological Sciences*
468 282:20151952.
- 470 Pollock, L. J., W. K. Morris, and P. A. Vesk. 2012. The role of functional traits in species
distributions revealed through a hierarchical model. *Ecography* 35:716–725.
- 472 Quental, T. B., and C. R. Marshall. 2013. How the Red Queen Drives Terrestrial Mammals to
Extinction. *Science* 341:290–292.
- 474 Royle, J. A., and R. M. Dorazio. 2008. Hierarchical modeling and inference in ecology: the analysis
of data from populations, metapopulations and communities. Elsevier, London.
- 476 ———. 2012. Parameter-expanded data augmentation for Bayesian analysis of capture-recapture
models. *Journal of Ornithology* 152:521–537.
- 478 Royle, J. A., R. M. Dorazio, and W. a. Link. 2007. Analysis of Multinomial Models With Unknown
Index Using Data Augmentation. *Journal of Computational and Graphical Statistics* 16:67–85.
- 480 Royle, J. A., J. D. Nichols, M. Kéry, E. Ranta, and M. Kery. 2014. detection is of species when
Modelling occurrence and abundance imperfect 110:353–359.
- 482 Rubin, D. B. 1996. Multiple imputation after 18+ years. *Journal of the American Statistical
Assocaition* 91:473–489.
- Slater, G. J. 2015. Iterative adaptive radiations of fossil canids show no evidence for

- 484 diversity-dependent trait evolution. *Proceedings of the National Academy of Sciences*
112:4897–4902.
- 486 Smits, P. D. 2015. Expected time-invariant effects of biological traits on mammal species duration.
Proceedings of the National Academy of Sciences 112:13015–13020.
- 488 Strömberg, C. A. E. 2005. Decoupled taxonomic radiation and ecological expansion of open-habitat
grasses in the Cenozoic of North America. *Proceedings of the National Academy of Sciences of*
490 *the United States of America* 102:11980–4.
- Tomiya, S. 2013. Body Size and Extinction Risk in Terrestrial Mammals Above the Species Level.
492 *The American Naturalist* 182:196–214.
- Valentine, J. W. 1969. Patterns of taxonomic and ecological structure of the shelf benthos during
494 Phanerozoic time. *Paleontology* 12:684–709.
- Wang, S. C., P. J. Everson, H. J. Zhou, D. Park, and D. J. Chudzicki. 2016. Adaptive credible
496 intervals on stratigraphic ranges when recovery potential is unknown. *Paleobiology* 42:240–256.
- Wang, S. C., and C. R. Marshall. 2016. Estimating times of extinction in the fossil record. *Biology*
498 *Letters* 12:20150989.
- Warton, D. I., B. Shipley, and T. Hastie. 2015. CATS regression - a model-based approach to
500 studying trait-based community assembly. *Methods in Ecology and Evolution* 6:389–398.
- Zachos, J. C., G. R. Dickens, and R. E. Zeebe. 2008. An early Cenozoic perspective on greenhouse
502 warming and carbon-cycle dynamics. *Nature* 451:279–283.
- Zachos, J. C., M. Pagani, L. Sloan, E. Thomas, and K. Billups. 2001. Trends, rhythms, and
504 aberrations in global climate 65 Ma to present. *Science* 292:686–693.

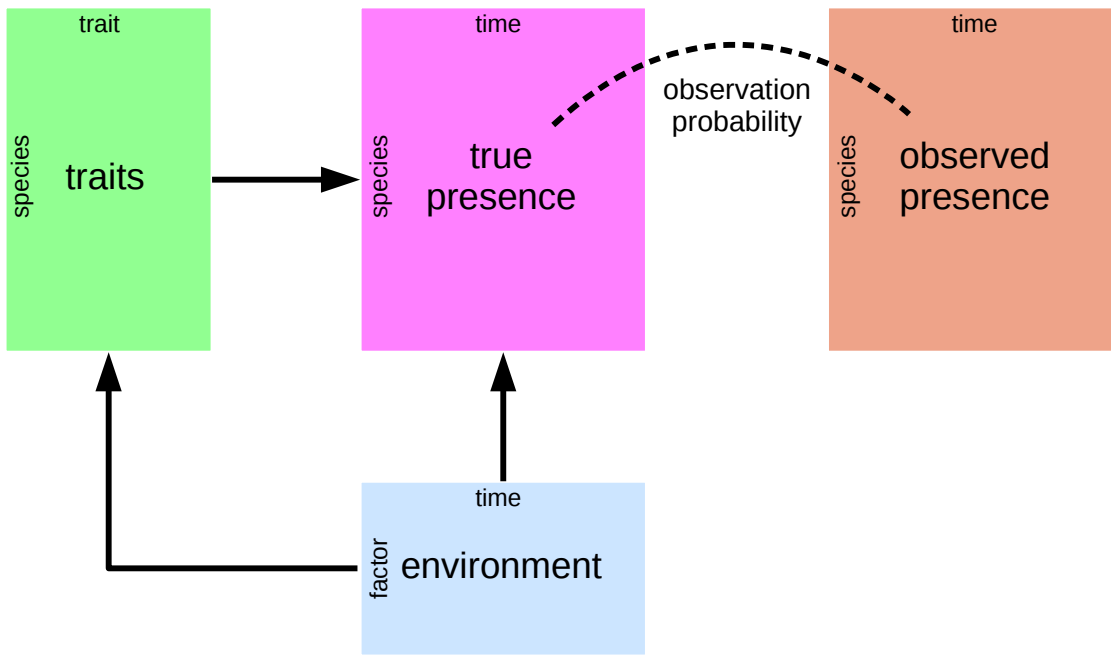


Figure 1: Conceptual diagram of the paleontological fourth corner problem. The observed presence matrix (orange) is the empirical presence/absence pattern for all species for all time points; this matrix is an incomplete observation of the “true” presence/absence pattern (purple). The estimated true presence matrix is modeled as a function of both environmental factors over time (blue) and multiple species traits (green). Additionally, the effect of environmental factors on species traits are also modeled as traits are expected to mediate the effects of a species environmental context. This diagram is based partially on material presented in Brown et al. (2014) and Warton et al. (2015).

	Time Bin							
	1	2	3	4	5	6	7	8
Observed	0	0	0	1	0	1	1	0
Certain	?	?	?	1	1	1	1	?
Potential	0	0	0	1	1	1	1	0
Potential	0	0	1	1	1	1	1	0
Potential	0	1	1	1	1	1	1	0
Potential	1	1	1	1	1	1	1	0
Potential	0	0	0	1	1	1	1	1
Potential	0	0	1	1	1	1	1	1
Potential	0	1	1	1	1	1	1	1
Potential	1	1	1	1	1	1	1	1

Figure 2: Conceptual figure of all possible occurrence histories for an observed species. The first row represents the observed presence/absence pattern for a single species at eight time points. The second row corresponds to the known aspects of the “true” occurrence history of that species. The remaining rows correspond to all possible occurrence histories that are consistent with the observed data. The process of parameter marginalization described in the text

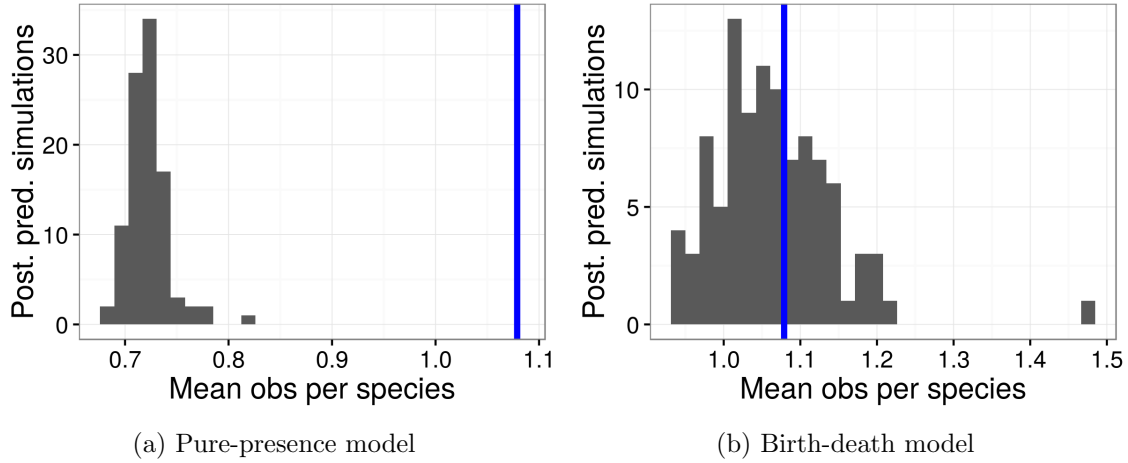


Figure 3: Comparison of the average observed number of occurrences per species (blue line) to the average number of occurrences from 100 posterior predictive datasets using the posterior estimates from the pure-presence and birth-death models.

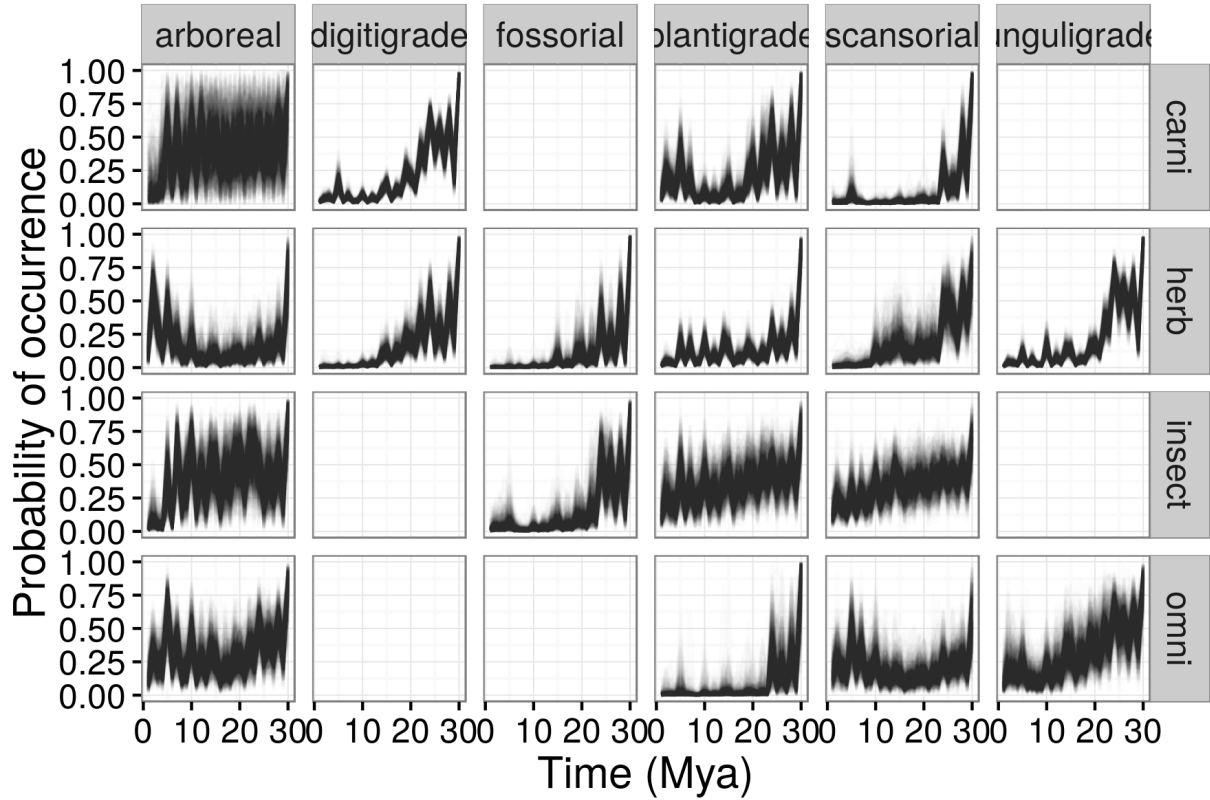


Figure 4: Probability of a mammal ecotype occurring over time as estimated from the pure-presence model. Each panel depicts 100 random samples from the model's posterior. The columns are by locomotor category and rows by dietary category; their intersections are the observed and analyzed ecotypes. Panels with no lines are ecotypes not observed in the dataset.

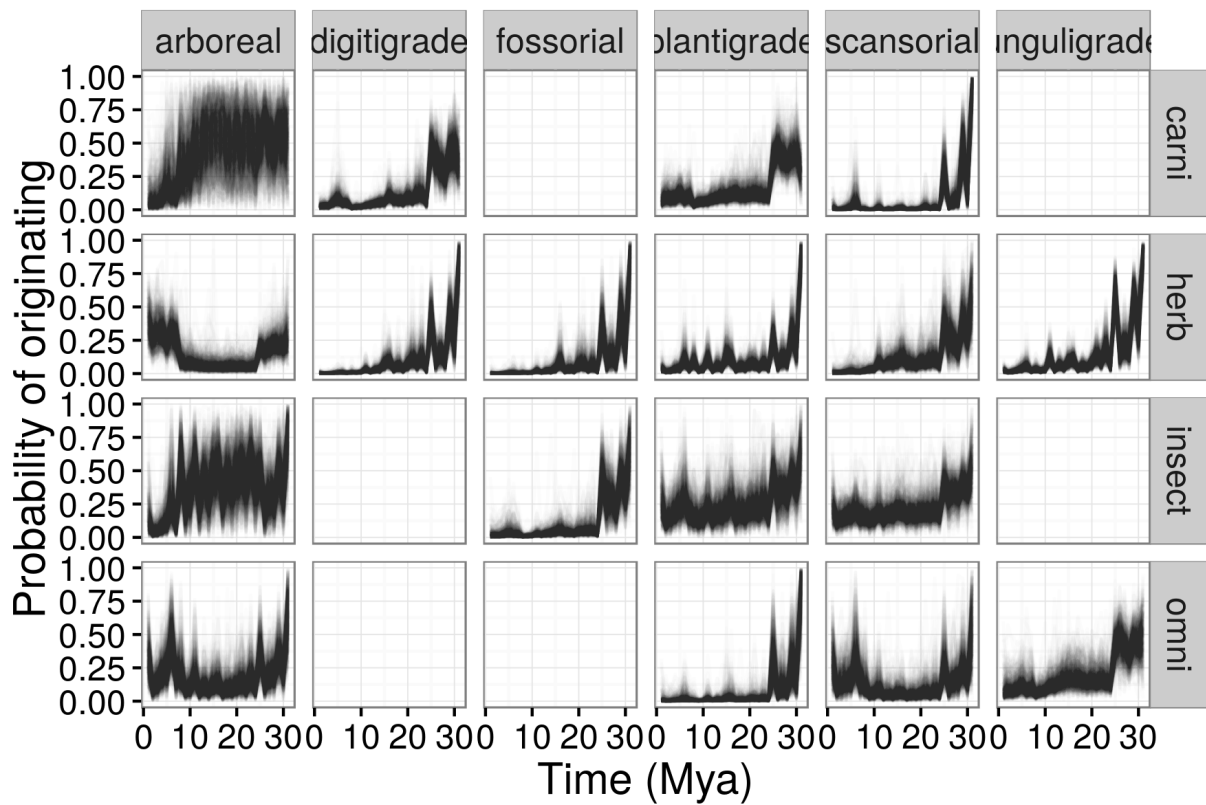


Figure 5: Probability of a mammal ecotype origination probabilities at each time point as estimated from the birth-death model. Each panel depicts 100 random samples from the model's posterior. The columns are by locomotor category and rows by dietary category; their intersections are the observed and analyzed ecotypes. Panels with no lines are ecotypes not observed in the dataset.

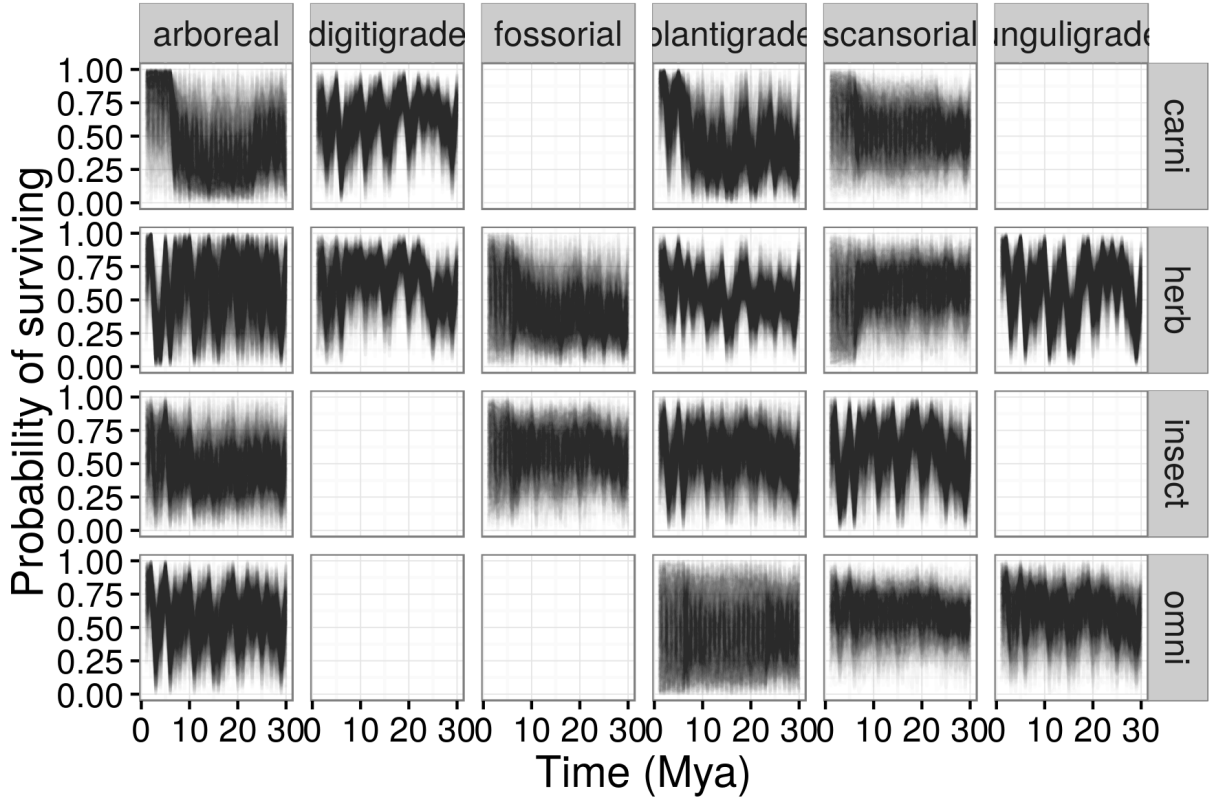


Figure 6: Probability of a mammal ecotype survival probabilities at each time point as estimated from the birth-death model. Each panel depicts 100 random samples from the model’s posterior. The columns are by locomotor category and rows by dietary category; their intersections are the observed and analyzed ecotypes. Panels with no lines are ecotypes not observed in the dataset.

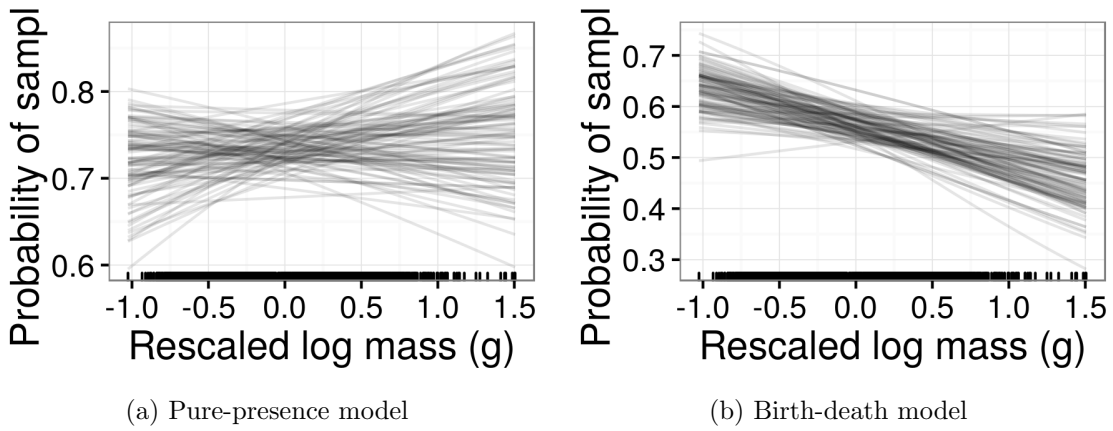


Figure 7: Estimates of the effect of species mass on probability of observing a present species (p). Mass has been log-transformed, centered, and rescaled; this means that a mass of 0 corresponds to the mean of log-mass of all observed species and that mass is in standard deviation units. Estimates are from both the pure-presence and birth-death models.

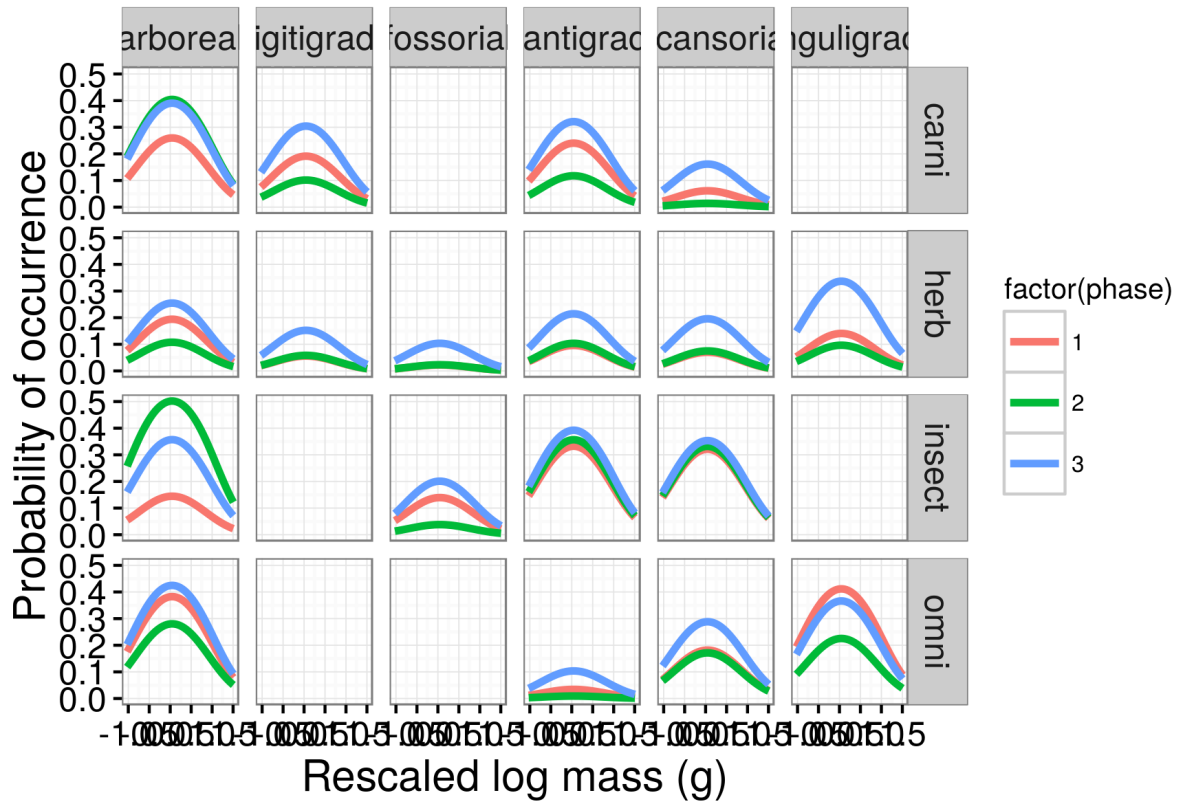


Figure 8: Mean estimate of the effect of species mass on the probability of a species occurrence for each of the three plant phases. The effect of mass is considered constant over time and that the only aspect of the model that changes with plant phase is the intercept of the relationship between mass and occurrence. The three plant phases are indicated by the color of the line. Mass has been log-transformed, centered, and rescaled; this means that a mass of 0 corresponds to the mean of log-mass of all observed species and that mass is in standard deviation units. Only the mean estimates of the effects of both mass and plant phase are plotted for clarity; these estimates are obviously made with uncertainty.

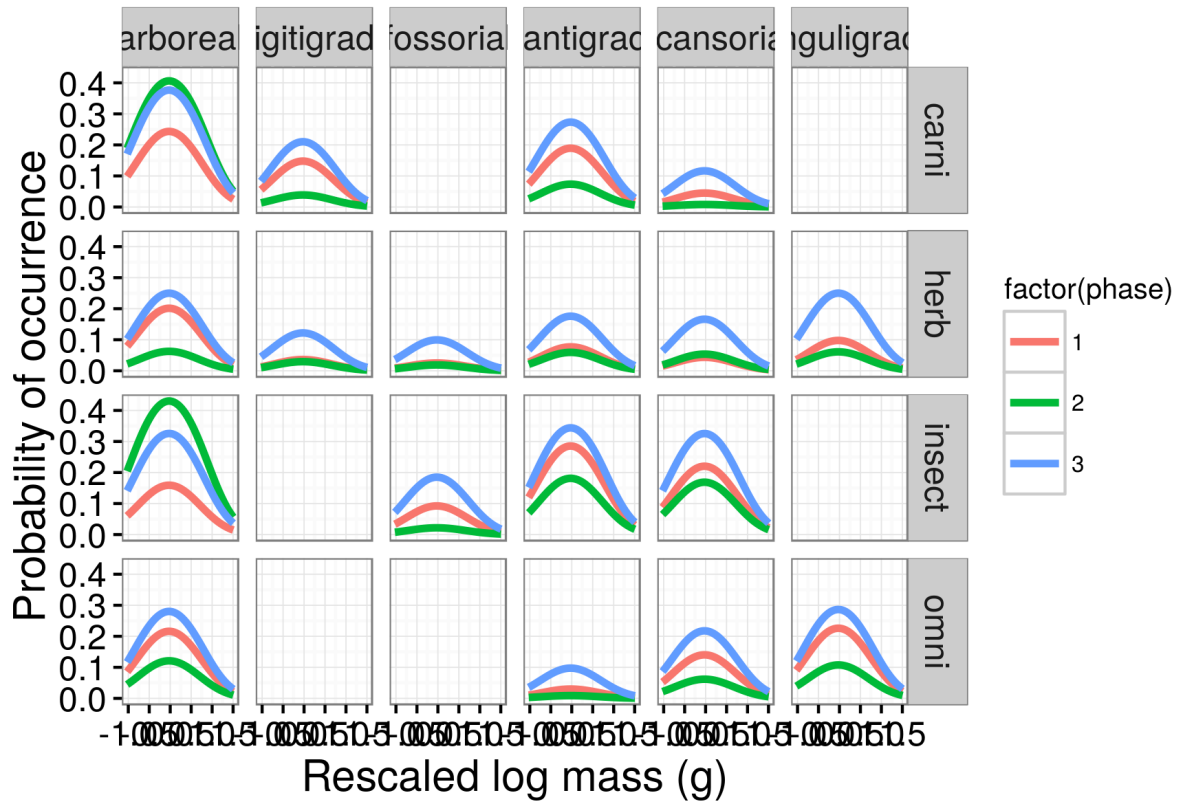


Figure 9: Mean estimate of the effect of species mass on the probability of a species originating for each of the three plant phases. The effect of mass is considered constant over time and that the only aspect of the model that changes with plant phase is the intercept of the relationship between mass and origination. The three plant phases are indicated by the color of the line. Mass has been log-transformed, centered, and rescaled; this means that a mass of 0 corresponds to the mean of log-mass of all observed species and that mass is in standard deviation units. Only the mean estimates of the effects of both mass and plant phase are plotted for clarity; these estimates are obviously made with uncertainty.

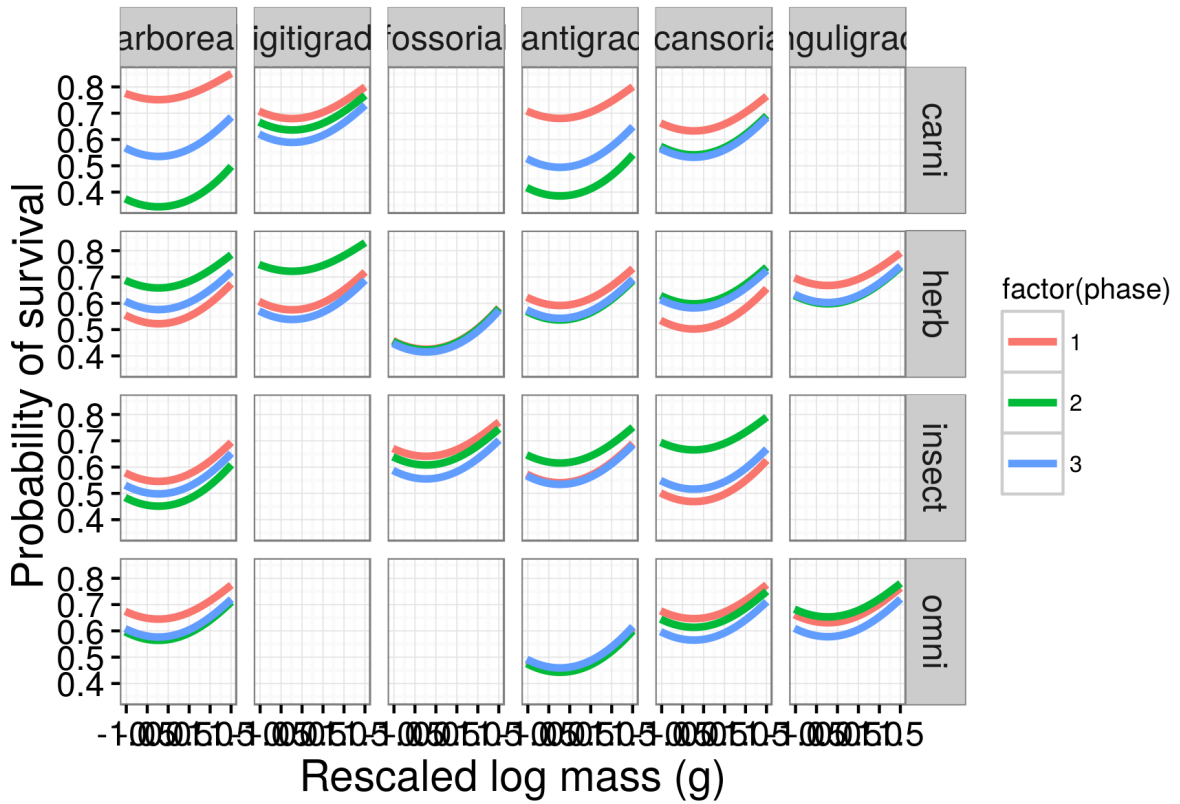


Figure 10: Mean estimate of the effect of species mass on the probability of a species survival for each of the three plant phases. The effect of mass is considered constant over time and that the only aspect of the model that changes with plant phase is the intercept of the relationship between mass and survival. The three plant phases are indicated by the color of the line. Mass has been log-transformed, centered, and rescaled; this means that a mass of 0 corresponds to the mean of log-mass of all observed species and that mass is in standard deviation units. Only the mean estimates of the effects of both mass and plant plant are plotted for clarity; these estimates are obviously made with uncertainty.

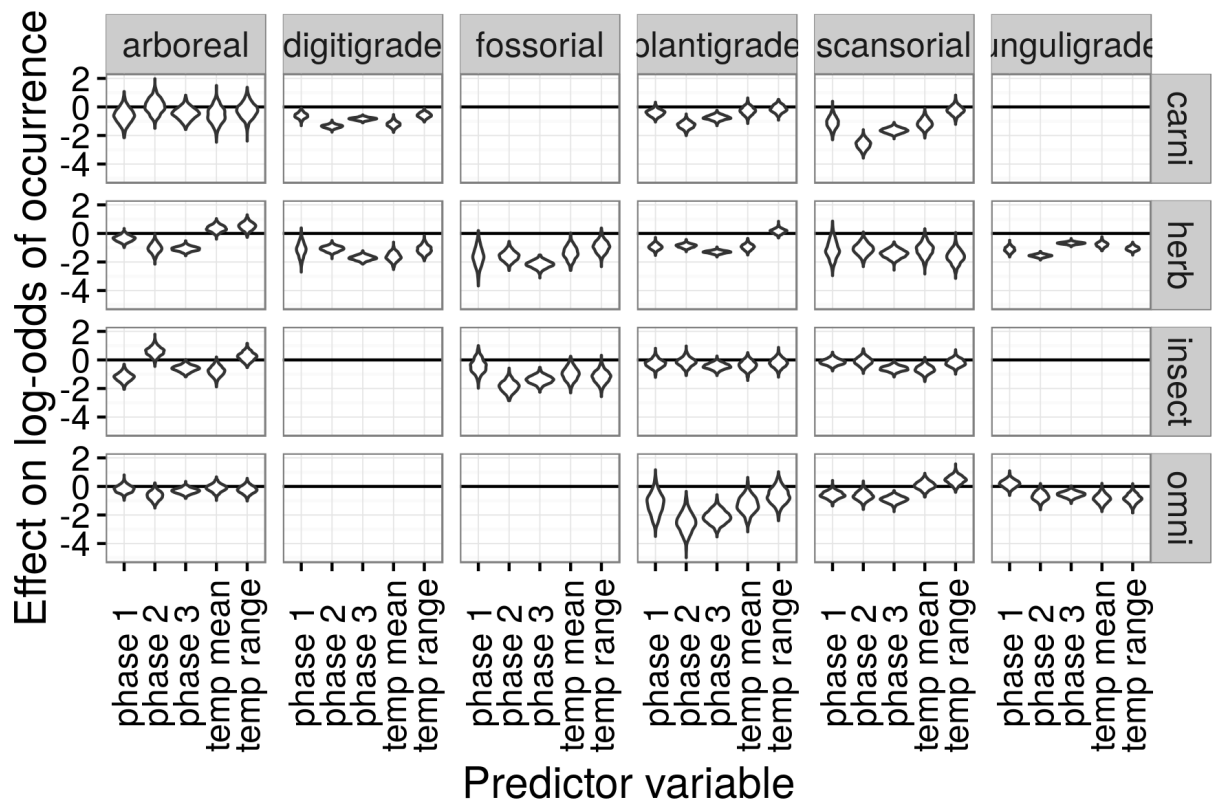


Figure 11: Estimated effects of the group-level covariates describing environmental context on log-odds of species occurrence. These estimates are from the pure-presence model.

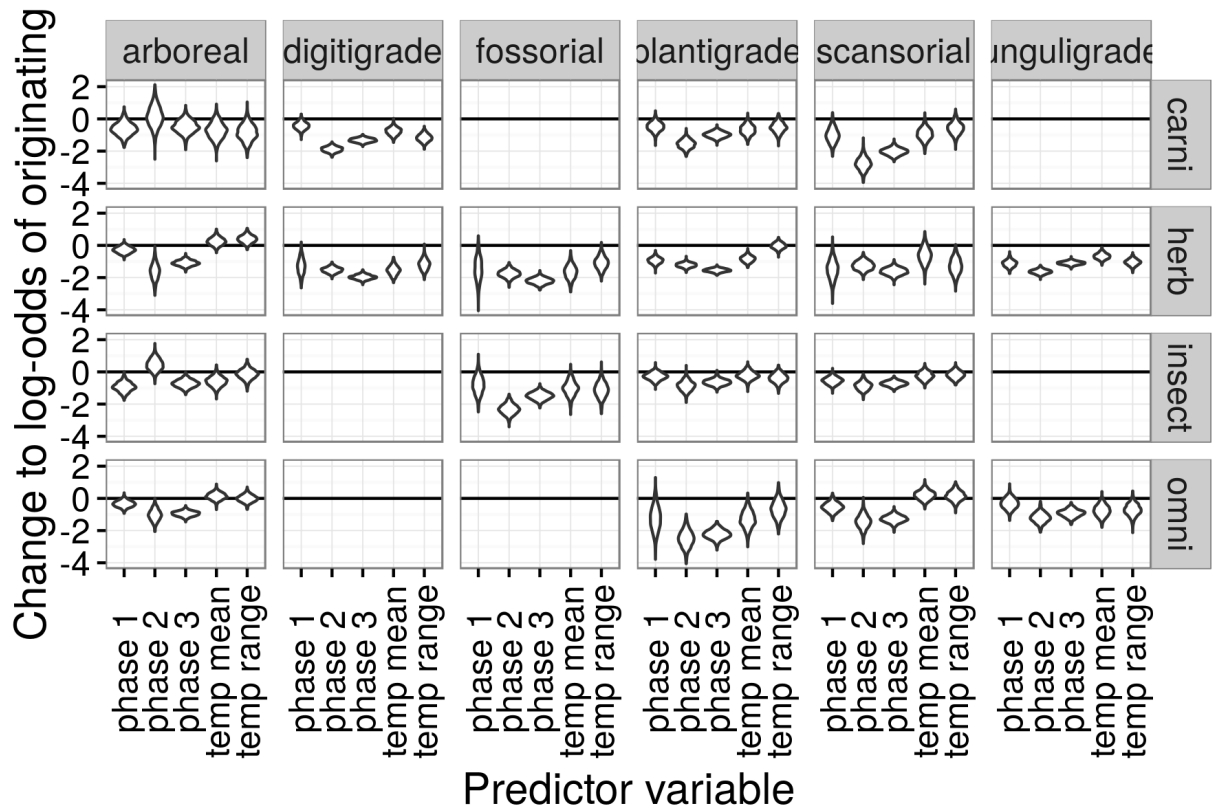


Figure 12: Estimated effects of the group-level covariates describing environmental context on log-odds of species origination. These estimates are from the birth-death model.

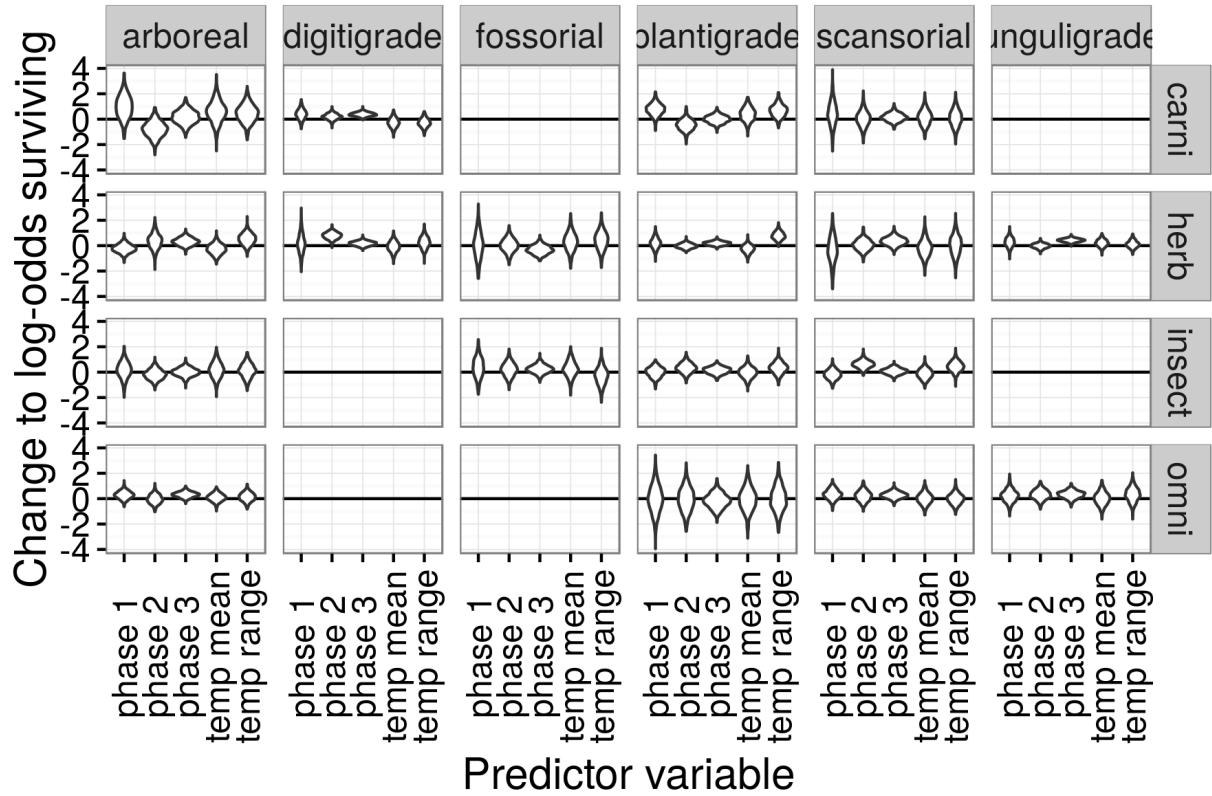


Figure 13: Estimated effects of the group-level covariates describing environmental context on log-odds of species survival. These estimates are from the birth-death model.

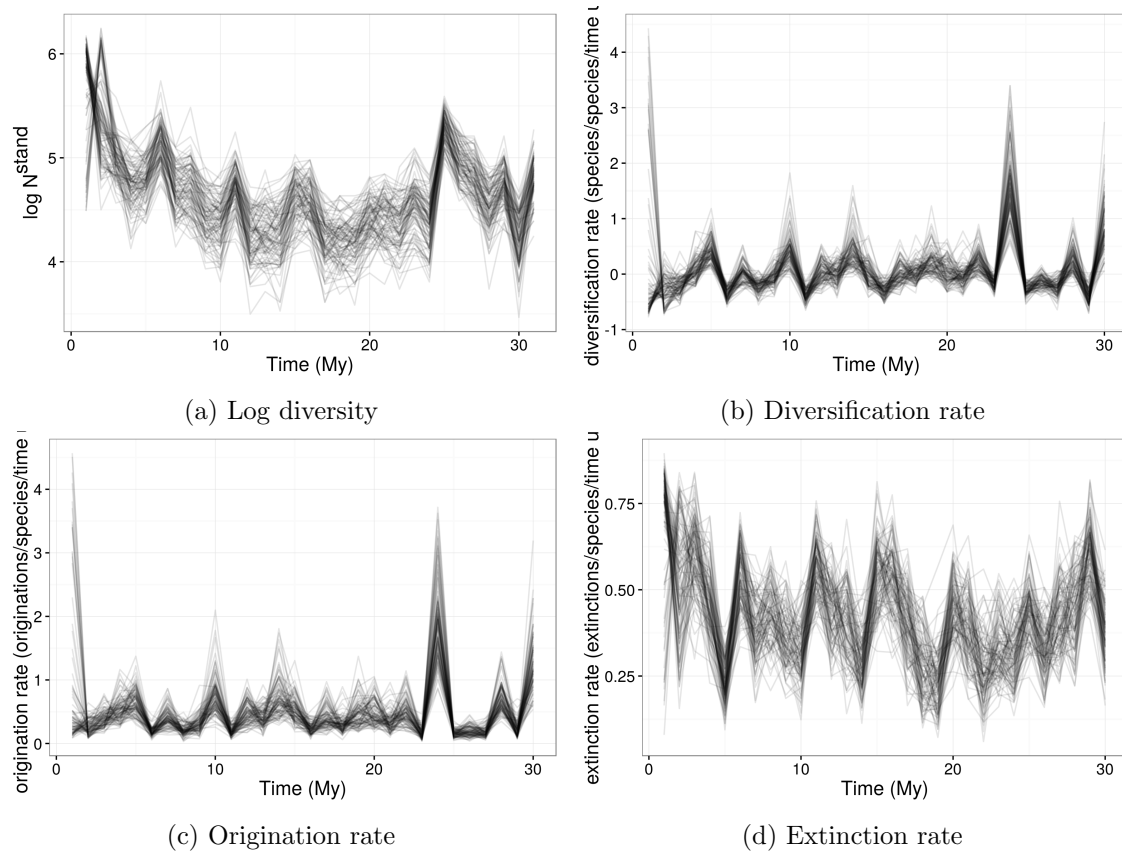


Figure 14: Posterior estimates of the time series of Cenozoic North American mammal diversity and its characteristic macroevolutionary rates; all estimates are from the birth-death model and 100 posterior draws are plotted to indicate the uncertainty in these estimates. The dramatic differences between diversity estimates at the first and second time points and the penultimate and last time points in this series are caused by well known edge effects in discrete-time birth-death models caused by $p_{-,t=1}$ and $p_{-,t=T}$ being partially unidentifiable (Royle and Dorazio, 2008); the hierarchical modeling strategy used here helps mitigate these effects but they are still present (Gelman et al., 2013; Royle and Dorazio, 2008). Diversification rate is in units of species gained per species present per time unit (2 My), origination rate is in units of species originating per species present per time unit, and extinction rate is in units of species becoming extinct per species present per time unit.

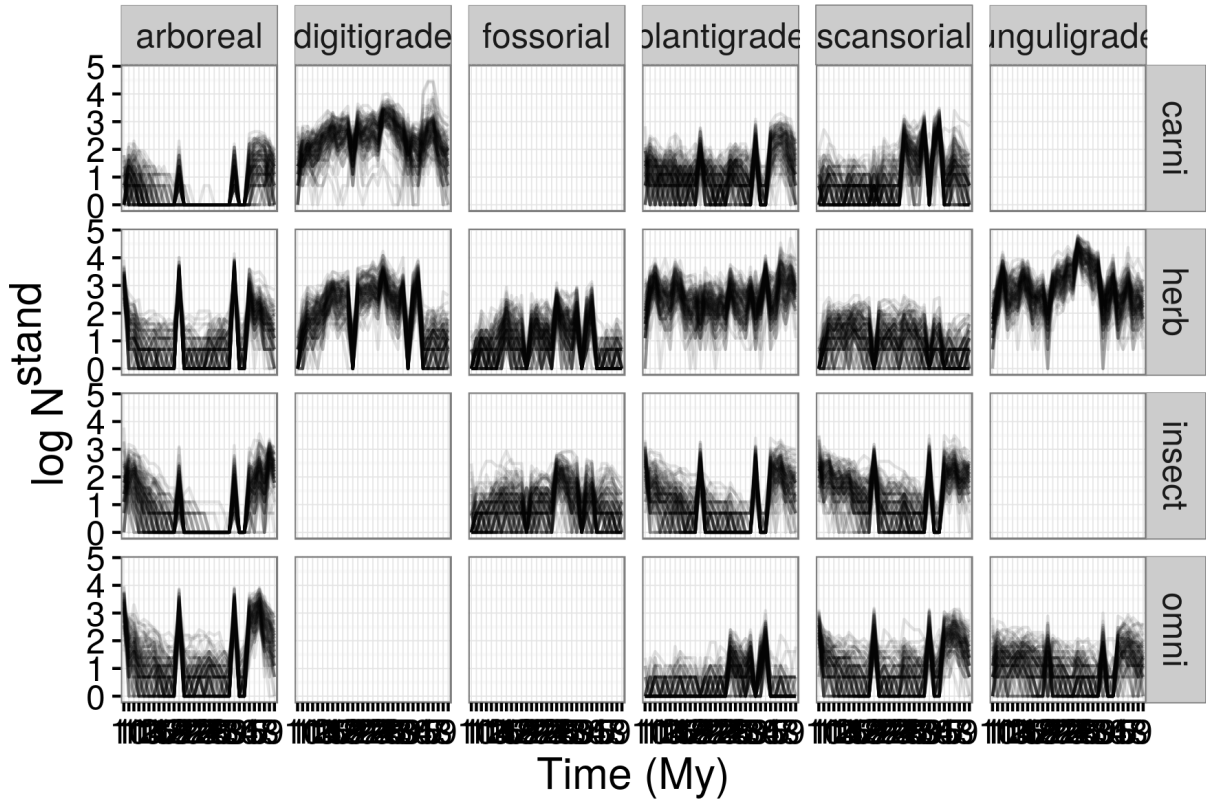


Figure 15: Posterior of standing log-diversity of North American mammals by ecotype for the Cenozoic as estimated from the birth-death model; 100 posterior draws are plotted to indicate the uncertainty in these estimates and what is technically plotted is log of diversity plus 1. The dramatic differences between diversity estimates at the first and second time points and the penultimate and last time points in this series are caused by well known edge effects in discrete-time birth-death models caused by $p_{-,t=1}$ and $p_{-,t=T}$ being partially unidentifiable (Royle and Dorazio, 2008); the hierarchical modeling strategy used here helps mitigate these effects but they are still present (Gelman et al., 2013; Royle and Dorazio, 2008).